

# ArcSin: Adaptive ranged cosine Similarity injected noise for Language-Driven Visual Tasks

Yang Liu<sup>1</sup>, Xiaomin Yu<sup>2</sup>, Gongyu Zhang<sup>1</sup>, Christos Bergeles<sup>1</sup>,  
Prokar Dasgupta<sup>1</sup>, Alejandro Granados<sup>1</sup>, Sebastien Ourselin<sup>1</sup>

<sup>1</sup>King’s College London <sup>2</sup>Qingdao University of Science and Technology

{yang.9.liu,firstname.secondname}@kcl.ac.uk, yuxm02@gmail.com

## Abstract

In this study, we address the challenging task of bridging the modality gap between learning from language and inference for visual tasks, including Visual Question Answering (VQA), Image Captioning (IC) and Visual Entailment (VE). We train models for these tasks in a zero-shot cross-modal transfer setting, a domain where the previous state-of-the-art method relied on the fixed scale noise injection, often compromising the semantic content of the original modality embedding. To combat it, we propose a novel method called Adaptive ranged cosine Similarity injected noise (ArcSin). First, we introduce an innovative adaptive noise scale that effectively generates the textual elements with more variability while preserving the original text feature’s integrity. Second, a similarity pool strategy is employed, expanding the domain generalization potential by broadening the overall noise scale. This dual strategy effectively widens the scope of the original domain while safeguarding content integrity. Our empirical results demonstrate that these models closely rival those trained on images in terms of performance. Specifically, our method exhibits substantial improvements over the previous state-of-the-art, achieving gains of 1.9 and 1.1 CIDEr points in S-Cap and M-Cap, respectively. Additionally, we observe increases of 1.5 percentage points (pp), 1.4 pp, and 1.4 pp in accuracy for VQA, VQA-E, and VE, respectively, pushing the boundaries of what is achievable within the constraints of image-trained model benchmarks. Code will be released.

## 1. Introduction

Vision and natural language processing (NLP) tasks are generally considered quite different. Recent approaches to use contrastive loss to train Vision-language (V&L) models have been a game changer in the field of multimodal learning [16, 32, 34], significantly narrowing the gap between image and text modalities and setting a new benchmark in

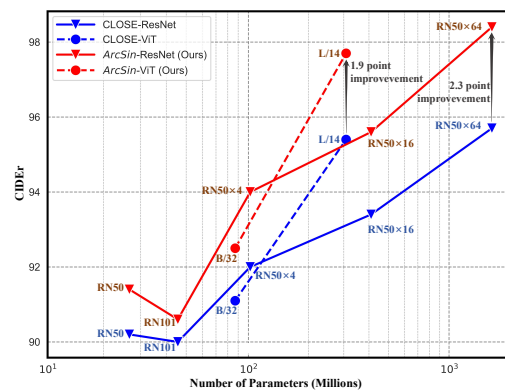


Figure 1. ArcSin surpasses state-of-the-art method CLOSE [12] in the Single Image Captioning (S-Cap) task, utilizing various CLIP models [32] as contrastive backbones for image-text feature alignment, while maintaining a consistent language model (T5-base [33]). The graph illustrates the relationship between the number of model parameters and corresponding CIDEr [38] scores.

multimodal integration and understanding. The modality gap, which highlights the disparity in feature distributions across different modalities, is a critical challenge in tasks like cross-modal retrieval and multimodal fusion [41, 48]. Recent efforts in domain adaptation have been instrumental in this regard, offering new perspectives and solutions [30]. The integration of cross-modal alignment techniques has further advanced the field, demonstrating significant improvements in handling multimodal data [25]. Moreover, the development of representation learning and feature fusion methods has been a cornerstone in bridging the modality gap, contributing to more robust and effective multimodal learning models [25, 30, 41, 48].

Despite these advances, zero-shot cross-modal transfer remains a relatively unexplored frontier. This is primarily due to the inherent disparities between image and text vectors in contrastive embeddings, which create a unique obstacle in achieving effective cross-modal communication

[7, 26]. Previous studies have explored various methods to bridge this modality gap. For instance, approaches like ViBERT [26] and UNITER [7] have shown considerable advancements in aligning visual and textual representations through joint training strategies. Studies such as [9, 10, 45] have demonstrated the effectiveness of noise injection in bolstering model robustness. Furthermore, works [12, 14] have successfully applied noise injection to enhance cross-modal transfer and generalization across diverse modalities.

However, the application of noise injection to close the modality gap presents a critical challenge: balancing the integrity of the original embedding with the need to bridge the gap between modalities. On the one hand, although injecting large amounts of noise can indeed bridge the gap between different modalities, it risks altering the semantic content of the injected feature. Such significant modifications can lead to a failure in accurately transferring the original semantic information to the other modality. On the other hand, injecting minimal noise while preserving semantic integrity often proves insufficient in effectively closing the modality gap. This delicate balance between domain gap reduction and semantic preservation is crucial for the successful application of noise injection techniques in multimodal learning. Our research addresses this dichotomy by developing a method that judiciously modulates the level of noise injection, ensuring both the closure of the modality gap and the retention of semantic fidelity.

We present a novel adaptive noise technique known as *Adaptive ranged cosine Similarity injected noise (ArcSin)*. This method effectively narrows the domain gap while preserving semantic integrity. By delving into the core concept of cosine similarity, *ArcSin* optimizes noise injection based on feature values, offering a more adaptable approach that aligns with the fundamental nature of features shaped by contrastive loss, which aims to maintain high similarity scores across different domains with comparable semantic content. Our innovations therefore represent a significant step forward in the nuanced and dynamic field of text-to-image transfer within multimodal learning.

To prove the effectiveness of our method, we have designed experiments on various language-driven vision-language tasks, which are trained exclusively on textual descriptions and utilize image inputs only during testing. This domain is economically viable and is rich in data availability, given the large repositories of text on the Internet. The vision-language tasks include Visual Question Answering (VQA), Image Captioning, and Visual Entailment. In VQA, whereby a model answers text-based questions about images [3, 11], our approach leverages text-only training to utilize extensive textual data, enhancing model robustness and generalizability. Similarly, in image captioning, where the goal is to generate descriptive text for images [39], our method aids in synthesizing more contextually relevant and

accurate descriptions. For visual entailment, which involves deducing the logical relationship between text and image [44]. As depicted in Fig. 1, our approach achieves enhanced performance across a range of contrastive models tasked with aligning text-image features, demonstrating that more advanced contrastive models contribute to improved results. This versatility not only marks a significant stride in academic research, such as point clouds [1], videos [46] and audio [8, 13, 43], but extends to practical applications, such as helping visually impaired individuals navigate their environments more effectively [4].

Our contributions are threefold. First, we introduce an adaptive noise injection technique and use a similarity threshold for refined control over noise application. This approach dynamically tunes the feature space based on similarity score and feature magnitude, ensuring that while the feature space diversifies to enable better domain generalization, the essence of the content remains intact. Second, we present an optimized noise injection strategy that broadens the noise scale without altering the similarity level with the original features. This innovation effectively expands the domain generalization potential. Finally, our method enhances the capabilities of existing contrastive-based models, like CLIP [32], by establishing a new framework for zero-shot cross-modal transfer. Via extensive experiments, we demonstrate that our method successfully bridges the modality gap, beating existing methods in reconciling feature distribution disparities between different modalities.

## 2. Related Work

### 2.1. Modality Gap in Multi-modal Learning

Vision and language (V&L) models trained with contrastive loss effectively close the modality gap by embedding text and images into vectors that align matching images and captions closely while distancing unrelated pairs [24]. This gap, identified as a geometric phenomenon in multi-modal models, arises from the interplay between model initialization and contrastive learning optimization [24]. Jiang *et al.* [17] and Qian *et al.* [31] further explored this by demonstrating that exact alignment is suboptimal for downstream tasks and advocating for the creation of meaningful latent modality structures, emphasizing the importance of considering label relationships in multi-modal data. Similarly, Udandarao *et al.* [36] studied the dynamics of class relationships within joint embedding spaces. Innovations like Flamingo [2] and Blip-2 [22] introduced novel cross-attention layers and efficient alignment methods, enhancing visual feature integration in language models. Building on these, Wang *et al.* [42] introduced the Connecting Multi-modal Contrastive Representations (C-MCR) approach, which encodes different modalities into a semantically aligned shared space, underscoring the importance of

semantic consistency in multi-modal learning. Our method complements these advancements by strategically injecting noise to bridge the modality gap, maintaining the integrity of original modality representations, and enhancing performance in downstream tasks through a nuanced and effective cross-modal understanding.

## 2.2. Noise Injection for Robust Representations

Noise injection has emerged as a key technique in enhancing robust representations and boosting generalization across various domains. The approach by Wang *et al.* [40] in deep neural networks for adversarial image detection highlights the role of noise in model robustness. This concept is further extended by Kaji and Kida [18], who demonstrate the efficacy of noise reduction in medical imaging, particularly in image-to-image translation, to improve image clarity and diagnostic accuracy. Similarly, the work of Ji *et al.* [15] integrates noise to enhance the realism of synthetic images, bridging the gap between synthetic and real-world data. Additionally, Zhen *et al.* [49] employs noise injection in flow-based generative models for brain imaging, facilitating data synthesis and modality translation.

In the vision-language sector, the innovative approach [12, 28, 35, 47] challenges traditional methods by learning visual tasks solely through language supervision. This is complemented by the efforts of [20], who demonstrate the effectiveness of noise injection in neural language generation models, underscoring its potential in natural language processing. Chen *et al.* [6] further enhances vision-language pre-training by incorporating noise to refine and distil data, proving the adaptability of the technique in zero-shot recognition tasks. Building upon these insights, our work introduces dynamic noise injection to close the modality gap between text and images, ensuring the similarity of augmented embeddings and advancing the field towards more cohesive multi-modal integration.

## 3. Problem Formulation

In this work, we define a visual task as a function  $f$  such that  $y = f(x_i, q)$ , where  $x_i$  denotes the visual input parameterized within a defined dimensional space, and  $q$  captures the task-specific directives, such as a query in Visual Question Answering (VQA) scenarios and a null value in Image Captioning (IC) contexts. The resultant  $y$  embodies the desired output, be it a response to a VQA prompt or a caption for a visual scene. Given the high cost of image annotation, our method focuses on training models using text data, denoted as  $x_t$ , and testing their performance on visual data, represented as  $x_i$ , which eliminates the need for labelled visual data. This training and testing paradigm assumes that text and image features are closely related in the model’s feature space. Vision-Language (V&L) models like CLIP [32], with their dual-encoders, text encoder

$E_t$  and image encoder  $E_i$ , have shown that aligning text and image features through contrastive loss can be effective. We use text embeddings  $e_t = E_t(x_t)$  for training and image embeddings  $e_i = E_i(x_i)$  for inference, ensuring that the model can interpret images based on what it has learned from the text, and the overview of our method is shown in Fig. 2.

## 4. Adaptive ranged cosine Similarity injected noise (*ArcSin*)

### 4.1. Adaptive Ranged Noise

Training with a mini-batch of encoded text features  $e_t \in \mathbb{R}^{B \times C}$ , where  $B$  and  $C$  represent the batch size and feature vector length respectively, we face the challenge of approximating these features to a visual domain in the absence of actual visual data. Accordingly, Our goal is not just to bridge the gap between different domains but to enhance the model’s ability to understand visual content through text-based training, and a natural idea is extending the text feature input domain. A simple heuristic consists of adding Gaussian noise to the text feature [12]. However, such undifferentiated noise will lead to changes in semantic information while expanding the domain. As shown in Fig. 3, we visualized the image feature deviation from the corresponding text feature, which is not equal for different text feature magnitudes. Our approach circumvents this by introducing Gaussian noise in a controlled manner that is mindful of content preservation, enhancing the domain generalization of the features while safeguarding the information they carry.

The essence of contrastive loss is to align similar content across varying domains through high cosine similarity. To effectively manage this, we draw parallels with a simplified two-dimensional scenario. Imagine a vector  $\vec{v}_0 = (\cdot, y_0)$  subject to a rotation by an angle  $\alpha$ . This rotation simulates the introduction of noise, with the constraint that the rotated vector’s similarity to the original remains above a certain threshold. The amount by which we can adjust  $y_0$  is hence limited, denoted by  $\delta(y_0)$ , to ensure that the inherent meaning within the data is not distorted.

As detailed in the left of Fig. 4, we derive bounds for positive and negative adjustments,  $\delta^+(y_0)$  and  $\delta^-(y_0)$ , which are defined as follows:

$$\delta^+(y_0) = \begin{cases} \sin(\arcsin(y_0) + \alpha) - y_0, & \arcsin(y_0) + \alpha < \frac{\pi}{2} \\ 1 - y_0, & \text{otherwise.} \end{cases} \quad (1)$$

$$\delta^-(y_0) = \begin{cases} \sin(\arcsin(y_0) - \alpha) - y_0, & \arcsin(y_0) - \alpha > -\frac{\pi}{2} \\ -1 - y_0, & \text{otherwise.} \end{cases} \quad (2)$$

These equations inform us of the range within which  $y_0$  can be altered without significantly changing the content,

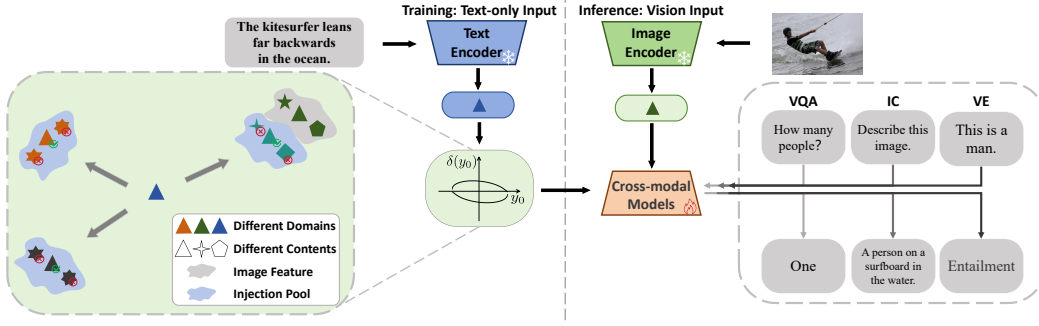


Figure 2. The *ArcSin* Architecture: In the training phase, textual descriptions are encoded to feature vectors using a pre-trained text encoder. These vectors are then augmented with dynamically injected noise, aligning them with vision-language tasks such as VQA, IC, and VE through task-specific prompts within the cross-modal models. During inference, images are processed into feature vectors via an image encoder, which then replaces the text-derived features, allowing the model to perform visual tasks using text-trained embeddings.

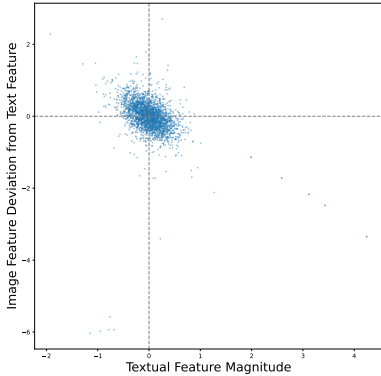


Figure 3. Illustration of the divergence between image and corresponding text features. We randomly selected 5 text-image feature pairs encoded by CLIP (ViT-B/32) [32] and visualized a set of  $512 \times 5$  points depicting value deviations. Here, the horizontal axis denotes the value of the text feature, while the vertical axis quantifies the deviation in the matching image feature, indicating variable deviations across different magnitudes of textual features.

and the curves are shown to the right of Fig. 4, which illustrate the varying degrees of permissible noise depending on the initial value of  $y_0$ .

Extending this principle back to our original high-dimensional feature space, the noise augmentation process for each feature dimension  $j$  is determined by its initial value  $e_t^j$ , following the mechanism:

$$\hat{e}_t^j = \begin{cases} e_t^j + \delta^+(e_t^j) \cdot \epsilon, & \epsilon \geq 0, \\ e_t^j - \delta^-(e_t^j) \cdot \epsilon, & \text{otherwise,} \end{cases} \quad (3)$$

where  $\delta^+$  and  $\delta^-$  are scaling functions derived from the bounds established by 2D Eqs. 1 and 2, and  $\epsilon \sim \mathcal{N}(0, 1)$  denotes the standard Gaussian distribution. We ensure inputs remain within  $[-1, 1]$  via a clamping function in line with feature value constraints (Algo. 1, line 7).

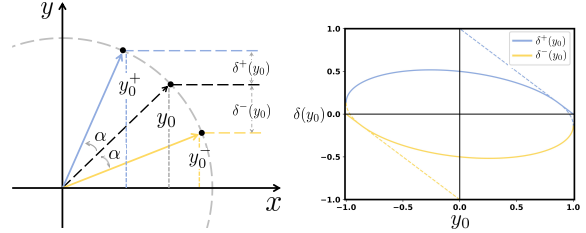


Figure 4. The visualization of permissible value deviations under a predefined similarity threshold in standard 2D space. **Left:** A vector (in black) with a vertical component  $y_0$ . Ensuring that the cosine similarity between the noise-augmented vectors (in blue and yellow) and the original vector remains above a certain threshold equates to confining rotation within an angle  $\alpha$ . The allowable positive and negative deviations are denoted by  $\delta^+(y_0)$  and  $\delta^-(y_0)$ , respectively. **Right:** The relationship between  $y_0$  and its potential deviations  $\delta(y_0)$ .

Our adaptive noise injection capitalizes on cosine similarity to adeptly generalize across new domains for multimodal features. It strikes a balance between domain expansion and content preservation, integral to effective model generalization.

## 4.2. Injection Pool

To balance content preservation with the introduction of variability, we carefully calibrate the noise injection scale. If we apply noise conservatively, we risk limiting the extent of domain generalization, potentially weakening the model’s ability to perform well across diverse domains. To address this, we introduce a novel, yet straightforward technique: the creation of a noise injection pool.

As shown in Algo. 1 (line 11-13), for each encoded text feature vector  $e_t$ , we generate  $N_p$  potential noise vectors. These vectors constitute our injection pool, a diverse set of candidates for domain generalization. We then experimentally add each noise vector to the original feature, comput-

ing the cosine similarity between the original  $e_t$  and noise-augmented version. The noise vector that yields the highest similarity is selected to create the final injected feature  $\hat{e}_t$ .

This method achieves two vital objectives: increase the magnitude of domain variation while maintaining the similarity score between the original and noise-injected features. Consequently, this elevates the likelihood of synthesizing features representative of a broader spectrum of domains, enhancing the model’s domain generalization capabilities.

### 4.3. Similarity Threshold Controlled Injection

To gain better control over the noise injection process, we employ a strategy governed by a predefined similarity threshold  $s$ . This threshold dictates the acceptable bounds of deviation from the original feature space during noise application. In practice, during training, we define an initial rotation angle  $\alpha$  within the interval  $[0, \frac{\pi}{2}]$  (Algo. 1, line 3), corresponding to the potential alteration in feature space.

Upon the arrival of a new mini-batch feature  $e_t$ , we select a random angle  $\alpha_0$  from within the predefined range. This angle serves as a pivot point to assess the average cosine similarity between the original feature  $e_t$  and the noise-enhanced feature  $\hat{e}_t$ . Based on the similarity score, As depicted in Algo. 1 (line 14-17), we dynamically adjust the angle bounds:

- If the similarity score falls below  $s - 0.01$ , we tighten the upper bound of  $\alpha$  to  $\alpha_0$ .
- On the contrary, if the similarity score exceeds  $s + 0.01$ , we expand the lower bound of  $\alpha$  to  $\alpha_0$ .
- If the score is within the threshold range, no changes.

This iterative adjustment ensures that the noise we introduce stays within a range that preserves content fidelity, as indicated by our similarity metric, while still providing sufficient variability for robust domain generalization.

## 5. Experiments

### 5.1. Datasets and Settings

To demonstrate the effectiveness of our model, we conducted experiments on three vision-language tasks: Image Captioning (IC), Visual Question Answering (VQA), and Visual Entailment (VE).

#### 5.1.1 Datasets

**Image Captioning (IC).** For the Image Captioning task, we employed the Karpathy split [19] to partition the COCO Captioning [5] dataset. During the training process, only the textual data from the training set was utilized to train the text generation model. We defined two training scenarios: Single Captioning (S-Cap) and Multiple Captioning (M-Cap). In Single Captioning, we selected a single text caption as both the input text and the target output text. In

---

### Algorithm 1: Adaptive Ranged Cosine Similarity Injected Noise (*ArcSin*) (Sec. 4)

---

**Input:** Encoded text features  $e_t \in \mathbb{R}^{B \times C}$ , similarity threshold  $s$ , noise pool size  $N_p$

**Output:** Noise-augmented text features  $\hat{e}_t$

```

1 Class ArcSin():
2   def __init__(s, Np):
3     self.αr ← [0, π/2]; // Set initial angle range
4     self.s ← s; // Set similarity threshold
5     self.Np ← Np; // Set noise pool size
6   def forward(et):
7     et ← et.clamp(-1, 1); // Clamp features
8     α0 ← Random(self.αr); // Select random
          angle
          // Dynamic scale calculation for noise
9     δ+(et) ← (et + α0 <
          π/2)? sin(arcsin(et) + α0) - et : 1 - et;
10    δ-(et) ← (et - α0 >
          -π/2)? sin(arcsin(et) - α0) - et : -1 - et;
          // Generate noise pool and augment features
11    Pn ← GenerateNoisePool(B, self.Np, C);
12    Ê ← et + Pn × ((Pn > 0)?δ+(et) :
          (-δ-(et)));
          // Select best noise vector based on similarity
13    êt ← arg max Sim(et, Ê);
          // Update angle range based on similarity
14    if AverageSim(et, êt) < s - 0.01 then
15      | self.αr.upper ← α0;
16    else if AverageSim(et, êt) > s + 0.01 then
17      | self.αr.lower ← α0;
18    return êt; // Return augmented feature

```

---

M-Cap, considering that an image may have multiple distinct caption descriptions, we used different captions about the same image as input and target output text. Through Multiple Captions, the model was able to learn captions of the same image in various contexts, thereby endowing the generated image captions with a more diverse range of contexts and expressions.

**Visual Question Answering (VQA).** For the VQA task, as we cannot access image information, we opt to use sentences containing scene descriptions as substitutes during training. Thus, in the training process, we utilize data that includes scene descriptions, questions, and target answers. We employ two datasets: VQA 2.0 [11] and VQA-E [23]. In VQA 2.0, we pair image captions from COCO Captioning with questions about the same images, enabling the model to comprehend visual scenes through textual descriptions. To address potential scenarios in which questions in the VQA 2.0 dataset involve details not present in the image

Task	Model	Text-only	S-Cap		M-Cap		VQA	VQA-E	VE
			B@4	C	B@4	C	Acc	Acc	Acc
Cap	ESPER Style [47]	✓	-	-	21.9	78.2	-	-	-
	CapDec [28]	✓	-	-	26.4	91.8	-	-	-
VQA	TAP-C [35]	✓	-	-	-	-	38.7	-	-
	BLIP-2 ViT-G OPT 6.7B [22]	zero-shot	-	-	-	-	52.6	-	-
	Flamingo 80B [2]		-	-	-	-	56.3	-	-
VE	CLIP Cls. [35]	✓	-	-	-	-	-	-	66.6
All	W/o Noise	✓	4.2	16.4	21.9	68.7	60.2	59.8	68.2
	CLOSE [12]	✓	28.2	95.8	29.6	98.5	61.3	63.4	74.6
	<i>ArcSin</i> (Ours)	✓	<b>29.4</b>	<b>97.7</b>	<b>30.3</b>	<b>99.6</b>	<b>61.8</b>	<b>64.8</b>	<b>76.0</b>
	W/Image (Upper bound)		34.4	113.2	34.4	113.2	65.4	67.9	77.7

Table 1. Comparison with previous work on different V&L tasks. Most of them are proposed for specific tasks, and only CLOUSE and our *ArcSin* can process all the provided tasks. We report BLEU-4 and CIDEr scores for S-Cap and M-Cap, and accuracy percentages for VQA, E-VQA and VE. ‘zero-shot’ indicates training on other datasets within images. we take training within images as the upper bound. The highest scores are in bold.

captions, we use the VQA-E dataset. This dataset is a subset of VQA 2.0, with captions from COCO Captioning verified to contain answers to the questions. This ensures that during training, questions can be answered solely through text. We evaluated the model separately on the VQA 2.0 test-dev set and the VQA-E validation set. These two settings will be called ‘VQA’ and ‘VQA-E’, respectively.

**Visual Entailment (VE).** This task aims to determine whether there is an entailment, contradiction, or neutral relationship between a given image of a premise and a hypothesis sentence. Since images cannot be obtained during training, we choose to use textual premises as substitutes. We conducted training using the SNLI[27] dataset and evaluated the model on the SNLI-VE[11] dataset.

### 5.1.2 Implementation Details

Our experiments were carried out on a single NVIDIA Tesla V100 GPU. For encoding text and image inputs, we utilized the CLIP L/14 model [32] to generate 768-dimensional feature embeddings. During training, these embeddings were kept static. Our training procedure involved augmenting the text features with our novel noise injection technique, where the scale of noise injection was regulated using a cosine similarity threshold  $s$  equal to 0.24, 0.55, 0.65, 0.52 and 0.5 in S-Cap, M-Cap, VQA, VQA-E and VE respectively, which was fine-tuned according to the performance of the validation set. To expand the diversity of the feature space, we constructed a pool of  $N = 100$  potential injections, selecting the feature with the highest similarity for each instance. Subsequent processing of these features was carried out by the pre-trained T5-base model [33]. We fine-tune our model with Adam optimizer [21] with a linear decaying learning rate starting at  $3e - 4$ ,  $\beta_1 = 0.9$ , and  $\beta_2 = 0.999$ . We use the beam search with a beam size 5 for

the evaluations to keep the same as [12]. For batch size, we standardized 128 except M-Cap, which used a batch size of 32. Training durations were set to 10 epochs for all tasks, except VQA-E, which required 20 epochs. During inference, we replaced text features with image features, facilitating the model’s application to visual input.

### 5.1.3 Metrics

For the IC task, we primarily use CIDEr [38] and BLEU-4 [29] as evaluation metrics. CIDEr focuses on assessing the consistency between generated captions and reference captions, while BLEU-4 is employed to measure the n-gram matching degree between generated captions and reference captions. For the VQA task, Accuracy serves as the primary evaluation metric. This metric quantifies the proportion of model-generated answers that match the ground-truth answers, providing a comprehensive understanding of the overall accuracy of the model in answering questions related to a given scene image. For the VE task, Accuracy is also employed as the main evaluation metric. Accuracy is used to gauge the model’s precision in correctly determining the relationship between the premise image and the hypothesis sentence, offering a clear assessment of the model’s performance.

## 5.2. Comparison with State-of-the-art Methods

To evaluate the efficacy of the proposed *ArcSin*, we carried out a series of comparative experiments against a comprehensive suite of state-of-the-art models across a diverse array of visual tasks. These tasks include Image Captioning (IC) in both its multiple captioning (M-Cap) and single captioning (S-Cap) variants, Visual Question Answering (VQA and VQA-E) and Visual Entailment (VE). The outcomes of these experiments are summarized in Tab. 1. For the



Figure 5. t-SNE [37] visualization of noise-injected features from various methods. With a fixed cosine similarity of 0.4, we analyzed 400 image-text pairs (shown as red-blue points). Our *ArcSin* is illustrated by orange points, which show the extended domain coverage that promotes the learning of more general features. On the contrary, green points illustrate noise-injected features of CLOSE [12], which display minimal variation in text features, resulting in a constrained augmentation effect.

CLOSE method, we utilized the publicly available source code<sup>1</sup> for our implementation, noting that some of our results surpassed those reported in their original study, while others fell short. This discrepancy was consistent between three different server environments, suggesting robustness in our findings. Most of these methods can only process specific V&L tasks except CLOSE and our *ArcSin*, so we will focus more on these two methods. A noteworthy observation in both CLOSE and *ArcSin* is the substantial performance enhancement compared to the approach of direct training with text data without noise enhancement. This underscores the significant domain gap that persists between the features of the image and the text, despite the concerted efforts of contrastive models such as CLIP [32] to bridge this gap. Within the limitation of the upper bound that the image-trained model, our method shows a remarkable improvement over CLOSE, with gains of 1.9 and 1.1 CIDEr points in S-Cap and M-Cap, respectively, and increases of 1.5 pp (percentage points), 1.4 pp, and 1.4 pp in accuracy for VQA, VQA-E and VE, respectively.

Fig. 5 provides a comparative visualization of text and image features, as well as the augmented text features by CLOSE and our *ArcSin*, both calibrated to similar levels of similarity with the original text feature. The diagram highlights a clear gap between text and image features, a division that persists regardless of their content similarities. Within identical domains, however, we observe content

Method	M-Cap		VQA-E	VE
	B@4	C	Acc	Acc
Fixed Scale Noise (CLOSE)	29.6	98.5	63.4	74.6
Adaptive Ranged Injection	30.0	99.3	<b>64.8</b>	75.5
Adaptive Ranged Injection + Injection Pool (Ours)	<b>30.3</b>	<b>99.6</b>	<b>64.8</b>	<b>76.0</b>

Table 2. The results of different components of *ArcSin* on M-Cap, VQA-E, and VE. BLEU-4 and CIDEr scores are reported on M-Cap, and accuracy percentage is reported on VQA-E and VE.

variations are more densely grouped. This observation implies that the demarcation in feature space is predominantly influenced by the domain gap. In particular, *ArcSin* delineates its features with a greater degree of separation from those modified by CLOSE. As such, our method demonstrates an enhanced ability to bridge diverse domains compared to CLOSE. The level of similarity, influenced by both domain gap and content differences, indicates that *ArcSin* successfully achieves broader domain generalization while preserving content fidelity. Additionally, although the visual representation in the manuscript of CLOSE may imply injected feature can comprehensive coverage of the image domain, such a breadth of coverage presumably requires extensive application of Gaussian noise. This can lead to substantial alterations in content and potentially diminish performance. Our target, however, aims to achieve extending generalization across various domains while minimizing content distortions. This strategy enhances the adaptability of our models to a wider array of domains, including images. As illustrated in Fig. 6, *ArcSin* exhibits a more precise understanding of the image content.

### 5.3. Ablation Study

**Performance Analysis of Different Components in *ArcSin*.** In light of our method outperforming state-of-the-art approaches across various tasks, we undertook an ablation study to dissect the impact of the individual components within our proposed framework. Tab. 2 presents a comparative analysis, illustrating that our adaptive noise injection method yields superior results over the fixed-scale noise approach previously suggested by [12]. While the inclusion of an injection pool offers incremental gains, it is the adaptability of our injection technique that stands out as the pivotal factor in enhancing performance. This indicates that while both refining the injection process and expanding the injection space contribute to addressing modality shift challenges, optimizing the injection methodology plays a more decisive role.

**The Effects of Different Backbones.** In this work, we employ the CLIP model with the ViT-L/14 configuration for aligning image and text features, and the T5-base model to process these features, as established by the CLOSE framework. To explore the influence of various architectural designs and substantiate the robustness of *ArcSin*, we systematically evaluated a suite of CLIP and T5 models, with the

<sup>1</sup><https://github.com/allenai/close/tree/main>

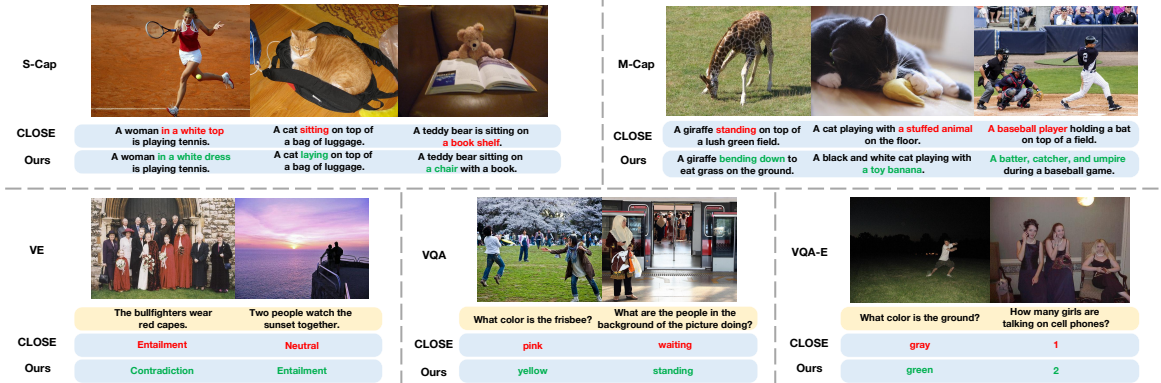


Figure 6. Qualitative comparisons with state-of-the-art method CLOSE [12] on some cases from 3 different vision-language tasks, including Cap (S-Cap and M-Cap), VE, and VQA (VAQ and VQA-E).

CLIP Model	T5 Model	S-Cap		VQA-E
		B@4	C	Acc
ViT-L/14	small	29.0	95.7 (1.3↑)	63.3 (4.4↑)
ViT-L/14	base	29.4	97.7 (1.9↑)	64.8 (1.4↑)
ViT-L/14	large	28.2	96.4 (2.5↑)	64.5 (0.7↓)
ViT-B/32	base	27.9	92.5 (1.4↑)	62.4 (1.0↑)
RN101	base	27.2	90.6 (0.6↑)	61.7 (1.9↑)
RN50	base	27.9	91.4 (1.2↑)	61.5 (1.1↑)
RN50×4	base	28.1	94.0 (2.0↑)	63.0 (1.5↑)
RN50×16	base	28.3	95.6 (2.2↑)	63.6 (1.1↑)
RN50×64	base	<b>29.7</b>	<b>98.4 (2.3↑)</b>	<b>65.3 (1.1↑)</b>

Table 3. Performance comparison of various contrastive and language backbone models utilizing *ArcSin*. The table outlines the contrastive models and language models in the first two columns, respectively, while the subsequent columns report the BLEU-4 and CIDEr scores for S-Cap and accuracy percentages for VQA-E. Notably, the value within parenthesis indicates the performance differential relative to CLOSE [12], with a green upward arrow (↑)/red downward arrow (↓) denoting improvement/reduction.

comparative results presented in Tab. 3. Our analysis reveals that superior contrastive backbones generally lead to improved performance, highlighting the importance of effective image-text alignment. With consistent use of the T5-base model, the RN101 variant was identified as the least effective in extracting features. Meanwhile, the T5-base model outperformed the T5 large model when paired with the ViT-L/14 CLIP model, suggesting that an increase in language model complexity does not invariably result in performance gains and may even cause overfitting to textual data. In addition, *ArcSin* demonstrated notable enhancements over CLOSE across all tested backbones except one, affirming the robustness and superior performance of our proposed method.

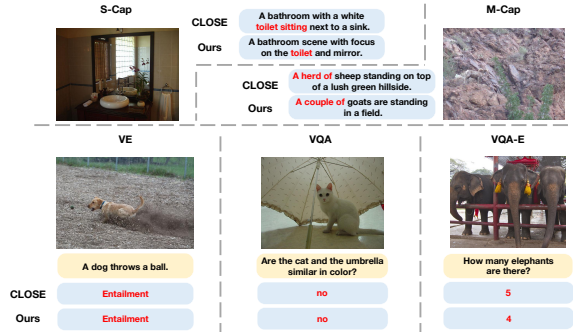


Figure 7. Some failure cases. *ArcSin* does not perform well in disentangling and interpreting nuanced details, and distinguishing similar foreground and background elements.

## 6. Conclusion

In this work, we proposed an effective adaptive noise injection method *ArcSin*, tailored for language-driven visual tasks. *ArcSin* strategically enhances text features by perturbing them into varied domains, meticulously preserving content integrity. Besides, our refined noise injection strategy judiciously selects high-quality augmentations, thereby indirectly broadening the scope of injection and augmenting domain diversity. This dual-faceted approach synergistically consolidates into a powerful and resilient method, setting new benchmarks across a range of visual tasks and network architectures. The superiority of our *ArcSin* over existing methods is evident, although it does encounter challenges with certain intricate visual features. As illustrated in Fig. 7, the method sometimes struggles to disentangle and interpret nuanced details or distinguish between similar foreground and background elements. However, we are confident that the exploration of language-driven visual tasks will catalyze the development of more sophisticated techniques. Future research efforts will be aimed at enhancing the comprehension of visual features through exclusively text-based learning. We



believe the insights garnered from this study will pave the way for more robust and nuanced strategies in the field.

## References

- [1] Mohamed Afham, Isuru Dissanayake, Dinithi Dissanayake, Amaya Dharmasiri, Kanchana Thilakarathna, and Ranga Rodrigo. CrossPoint: Self-Supervised Cross-Modal contrastive learning for 3D point cloud understanding. *arXiv preprint arXiv:2203.00680*, 2022. [2](#)
- [2] Jean-Baptiste Alayrac, Jeff Donahue, Pauline Luc, Antoine Miech, Iain Barr, Yana Hasson, Karel Lenc, Arthur Mensch, Katherine Millican, Malcolm Reynolds, et al. Flamingo: a visual language model for few-shot learning. *Advances in Neural Information Processing Systems*, 35:23716–23736, 2022. [2](#), [6](#)
- [3] Stanislaw Antol, Aishwarya Agrawal, Jiasen Lu, Margaret Mitchell, Dhruv Batra, C. Lawrence Zitnick, and Devi Parikh. Vqa: Visual question answering. In *Proceedings of the IEEE International Conference on Computer Vision (ICCV)*, pages 2425–2433, 2015. [2](#)
- [4] Jeffrey P. Bigham and Chandrika Jayant. Vizwiz: Nearly real-time answers to visual questions. *UIST: ACM Symposium on User Interface Software and Technology*, 2010. [2](#)
- [5] Xinlei Chen, Hao Fang, Tsung-Yi Lin, Ramakrishna Vedantam, Saurabh Gupta, Piotr Dollár, and C Lawrence Zitnick. Microsoft coco captions: Data collection and evaluation server. *arXiv preprint arXiv:1504.00325*, 2015. [5](#)
- [6] Xiaofei Chen, Yuting He, Cheng Xue, Rongjun Ge, Shuo Li, and Guanyu Yang. Knowledge boosting: Rethinking medical contrastive Vision-Language Pre-Training. *arXiv:2307.07246*, 2023. [3](#)
- [7] Yen-Chun Chen, Linjie Li, Licheng Yu, Ahmed El Kholy, Faisal Ahmed, Zhe Gan, Yu Cheng, and Jingjing Liu. Uniter: Universal image-text representation learning. In *European conference on computer vision*, pages 104–120. Springer, 2020. [2](#)
- [8] Benjamin Elizalde, Soham Deshmukh, Mahmoud Al Ismail, and Huaming Wang. CLAP: Learning audio concepts from natural language supervision. *ICASSP 2023-2023 IEEE International Conference on Acoustics, Speech and Signal Processing (ICASSP)*, 2023. [2](#)
- [9] Yunpeng Gong, Liqing Huang, and Lifei Chen. Person re-identification method based on color attack and joint defence. *CVPR workshop*, pages 4313–4322, 2021. [2](#)
- [10] Ian Goodfellow, Jean Pouget-Abadie, Mehdi Mirza, Bing Xu, David Warde-Farley, Sherjil Ozair, Aaron Courville, and Yoshua Bengio. Generative adversarial nets. *Advances in Neural Information Processing Systems*, 27:2672–2680, 2014. [2](#)
- [11] Yash Goyal, Tejas Khot, Douglas Summers-Stay, Dhruv Batra, and Devi Parikh. Making the v in vqa matter: Elevating the role of image understanding in visual question answering. In *Proceedings of the IEEE conference on computer vision and pattern recognition*, pages 6904–6913, 2017. [2](#), [5](#), [6](#)
- [12] Sophia Gu, Christopher Clark, and Aniruddha Kembhavi. I can’t believe there’s no images! learning visual tasks using only language data. *arXiv preprint arXiv:2211.09778*, 2022. [1](#), [2](#), [3](#), [6](#), [7](#), [8](#)
- [13] Andrey Guzhov, Federico Raue, Jörn Hees, and Andreas Dengel. AudioCLIP: Extending CLIP to image, text and audio. *arXiv preprint arXiv:2106.13043*, 2021. [2](#)
- [14] Feiran Huang, Alireza Jolfaei, and Akramul Azim. Robust multimodal representation learning with evolutionary adversarial attention networks. *IEEE Transactions on Evolutionary Computation*, 2021. [2](#)
- [15] Xiaozhong Ji, Yun Cao, Ying Tai, Chengjie Wang, Jilin Li, and Feiyue Huang. Real-world super-resolution via kernel estimation and noise injection. In *2020 IEEE/CVF Conference on Computer Vision and Pattern Recognition Workshops (CVPRW)*, pages 466–467. IEEE, 2020. [3](#)
- [16] Chao Jia, Yinfei Yang, Ye Xia, Yi-Ting Chen, Zarana Parekh, Hieu Pham, Quoc V. Le, Yun-Hsuan Sung, Zhen Li, and Tom Duerig. Scaling up visual and vision-language representation learning with noisy text supervision. *arXiv:2102.05918*, 2021. [1](#)
- [17] Qian Jiang, Changyou Chen, Han Zhao, Liquan Chen, Qing Ping, Son Dinh Tran, Yi Xu, Belinda Zeng, and Trishul Chilimbi. Understanding and constructing latent modality structures in multi-modal representation learning. *arXiv:2303.05952*, 2023. [2](#)
- [18] Shizuo Kaji and Satoshi Kida. Overview of image-to-image translation by use of deep neural networks: denoising, super-resolution, modality conversion, and reconstruction in medical imaging. *Radiological Physics and Technology*, 12(3): 235–248, 2019. [3](#)
- [19] Andrej Karpathy and Li Fei-Fei. Deep visual-semantic alignments for generating image descriptions. In *Proceedings of the IEEE conference on computer vision and pattern recognition*, pages 3128–3137, 2015. [5](#)
- [20] Chris Kedzie and Kathleen R. McKeown. A good sample is hard to find: Noise injection sampling and self-training for neural language generation models. In *Proceedings of the 12th International Conference on Natural Language Generation, INLG 2019, Tokyo, Japan, October 29 - November 1, 2019*, pages 584–593. Association for Computational Linguistics, 2019. [3](#)
- [21] Diederik P Kingma and Jimmy Ba. Adam: A method for stochastic optimization. *arXiv preprint arXiv:1412.6980*, 2014. [6](#)
- [22] Junnan Li, Dongxu Li, Silvio Savarese, and Steven Hoi. Blip-2: Bootstrapping language-image pre-training with frozen image encoders and large language models. *arXiv preprint arXiv:2301.12597*, 2023. [2](#), [6](#)
- [23] Qing Li, Qingyi Tao, Shafiq Joty, Jianfei Cai, and Jiebo Luo. Vqa-e: Explaining, elaborating, and enhancing your answers for visual questions. In *Proceedings of the European Conference on Computer Vision (ECCV)*, pages 552–567, 2018. [5](#)
- [24] Weixin Liang, Yuhui Zhang, Yongchan Kwon, Serena Yeung, and James Zou. Mind the gap: Understanding the modality gap in multi-modal contrastive representation learning. *arXiv:2203.02053*, 2022. [2](#)

- [25] Xiangbin Liu, Junping Du, M. Liang, and Ang Li. Cross-modal search method of technology video based on adversarial learning and feature fusion. *arXiv:2210.05243*, 2022. **1**
- [26] Jiasen Lu, Dhruv Batra, Devi Parikh, and Stefan Lee. Vilbert: Pretraining task-agnostic visiolinguistic representations for vision-and-language tasks. *Advances in neural information processing systems*, 32, 2019. **2**
- [27] Bill MacCartney and Christopher D Manning. Modeling semantic containment and exclusion in natural language inference. In *Proceedings of the 22nd International Conference on Computational Linguistics (Coling 2008)*, pages 521–528, 2008. **6**
- [28] David Nukrai, Ron Mokady, and Amir Globerson. Text-only training for image captioning using noise-injected clip. *arXiv preprint arXiv:2211.00575*, 2022. **3, 6**
- [29] Kishore Papineni, Salim Roukos, Todd Ward, and Wei-Jing Zhu. Bleu: a method for automatic evaluation of machine translation. In *Proceedings of the 40th annual meeting of the Association for Computational Linguistics*, pages 311–318, 2002. **6**
- [30] Fan Qi, Xiaoshan Yang, and Changsheng Xu. A unified framework for multimodal domain adaptation. *ACM Transactions on Multimedia Computing, Communications, and Applications*, 2018. **1**
- [31] Shengsheng Qian, Dizhan Xue, Quan Fang, and Changsheng Xu. Integrating Multi-Label contrastive learning with dual adversarial graph neural networks for Cross-Modal retrieval. *IEEE Trans. Pattern Anal. Mach. Intell.*, 45(4):4794–4811, 2023. **2**
- [32] Alec Radford and Jeff Wu. Learning transferable visual models from natural language supervision. *International Conference on Machine Learning*, 2021. **1, 2, 3, 4, 6, 7**
- [33] Colin Raffel, Noam Shazeer, Adam Roberts, Katherine Lee, Sharan Narang, Michael Matena, Yanqi Zhou, Wei Li, and Peter J Liu. Exploring the limits of transfer learning with a unified text-to-text transformer. *The Journal of Machine Learning Research*, 21(1):5485–5551, 2020. **1, 6**
- [34] Aditya Ramesh, Mikhail Pavlov, Gabriel Goh, Scott Gray, Chelsea Voss, Alec Radford, Mark Chen, and Ilya Sutskever. Zero-shot text-to-image generation. *arXiv:2102.12092*, 2021. **1**
- [35] Haoyu Song, Li Dong, Wei-Nan Zhang, Ting Liu, and Furu Wei. Clip models are few-shot learners: Empirical studies on vqa and visual entailment. *arXiv preprint arXiv:2203.07190*, 2022. **3, 6**
- [36] Vishaal Udandarao, Abhishek Maiti, Deepak Srivatsav, Suryatej Reddy Vyalla, Yifang Yin, and Rajiv Ratn Shah. COBRA: Contrastive Bi-Modal representation algorithm. *arXiv:2005.03687*, 2020. **2**
- [37] Laurens Van der Maaten and Geoffrey Hinton. Visualizing data using t-sne. *Journal of machine learning research*, 9 (11), 2008. **7**
- [38] Ramakrishna Vedantam, C Lawrence Zitnick, and Devi Parikh. Cider: Consensus-based image description evaluation. In *Proceedings of the IEEE conference on computer vision and pattern recognition*, pages 4566–4575, 2015. **1, 6**
- [39] Oriol Vinyals and Alexander Toshev. Show and tell: A neural image caption generator. *IEEE Conference on Computer Vision and Pattern Recognition*, 2015. **2**
- [40] Si Wang, Wenye Liu, and Chip-Hong Chang. Detecting adversarial examples for deep neural networks via layer directed discriminative noise injection. *2019 IEEE Asian Hardware-Oriented Security and Trust Symposium (Asian-HOST)*, 2019. **3**
- [41] Yang Wang, Meng Fang, Joey Tianyi Zhou, Tingting Mu, and D. Tao. Introduction to big multimodal multimedia data with deep analytics. *ACM Transactions on Multimedia Computing, Communications, and Applications*, 2021. **1**
- [42] Zehan Wang, Yang Zhao, Xize Cheng, Haifeng Huang, Jiageng Liu, Li Tang, Linjun Li, Yongqi Wang, Aoxiong Yin, Ziang Zhang, and Zhou Zhao. Connecting multi-modal contrastive representations. *arXiv:2305.14381*, 2023. **2**
- [43] Ho-Hsiang Wu, Prem Seetharaman, Kundan Kumar, and Juan Pablo Bello. Wav2CLIP: Learning robust audio representations from CLIP. *arXiv:2110.11499*, 2021. **2**
- [44] Ning Xie, Farley Lai, Derek Doran, and Asim Kadav. Visual entailment: A novel task for Fine-Grained image understanding. *arXiv preprint arXiv:1901.06706*, 2019. **2**
- [45] Qizhe Xie, Minh-Thang Luong, Eduard Hovy, and Quoc V Le. Self-training with noisy student improves imagenet classification. In *Proceedings of the IEEE/CVF conference on computer vision and pattern recognition*, pages 10687–10698, 2020. **2**
- [46] Hu Xu, Gargi Ghosh, Po-Yao Huang, Dmytro Okhonko, Armen Aghajanyan, Florian Metze, Luke Zettlemoyer, and Christoph Feichtenhofer. VideoCLIP: Contrastive pre-training for zero-shot Video-Text understanding. *arXiv preprint arXiv:2109.14084*, 2021. **2**
- [47] Youngjae Yu, Jiwan Chung, Heeseung Yun, Jack Hessel, JaeSung Park, Ximing Lu, Prithviraj Ammanabrolu, Rowan Zellers, Ronan Le Bras, Gunhee Kim, et al. Multimodal knowledge alignment with reinforcement learning. *arXiv preprint arXiv:2205.12630*, 2022. **3, 6**
- [48] Yefei Zhang, Yanjun Deng, Zhixin Zhou, Xianfei Zhang, Pengfei Jiao, and Zhidong Zhao. Multimodal learning for fetal distress diagnosis using a multimodal medical information fusion framework. *Frontiers in Physiology*, 2022. **1**
- [49] Xingjian Zhen, Rudrasis Chakraborty, Liu Yang, and Vikas Singh. Flow-based generative models for learning manifold to manifold mappings. In *Proceedings of the AAAI Conference on Artificial Intelligence*, pages 10711–10719. AAAI, 2020. **3**